Journal of Applied Fluid Mechanics, Vol. 9, No. 5, pp. 2053-2062, 2016.
Available online at www.jafmonline.net, ISSN 1735-3572, EISSN 1735-3645.

Effects of Temperature on the Wave Soldering of Printed Circuit Boards: CFD Modeling Approach

M. S. Abdul Aziz[1†], M. Z. Abdullah[1], C. Y. Khor[2], F. Che Ani[3, 4] and N. H. Adam[5]

[1] *School of Mechanical Engineering, Universiti Sains Malaysia, 14300 Nibong Tebal, Penang, Malaysia.*
[2]*Faculty of Engineering Technology (FETech), Universiti Malaysia Perlis (UniMAP), Level 1, Block S2, UniCITI Alam Campus, Sungai Chuchuh, 02100, Padang Besar, Perlis, Malaysia.*
[3]*Institute of Microengineering and Nanoelectronics, Universiti Kebangsaan Malaysia, 43600 Bangi, Selangor, Malaysia.*
[4]*Jabil Circuit Sdn. Bhd., Bayan Lepas Industrial Park, 11900, Bayan Lepas, Penang, Malaysia.*
[5]*Soil Instruments (M) Sdn Bhd, No. 12, Jln Utarid u5/14, Seksyen u5, Shah Alam, Selangor, Malaysia.*

†*Corresponding Author Email: sharizalaziz1983@gmail.com*

(Received July 1, 2014; accepted November 25, 2015)

ABSTRACT

This study investigated the effects of temperature on the wave soldering of printed circuit boards (PCBs) using three-dimensional finite volume analysis. A computational solder pot model consisting of a six-blade rotational propeller was developed and meshed using tetrahedral elements. The leaded molten solder (Sn63Pb37) distribution and PCB wetting profile were determined using the volume of fluid technique in the fluid flow solver, FLUENT. In this study, the effects of five different molten solder temperatures (456 K, 473 K, 523 K, 583 K, and 643 K) on the wave soldering of a 70 mm × 146 mm PCB were considered. The effects of temperature on wetting area, wetting profile, velocity vector, and full wetting time were likewise investigated. Molten solder temperature significantly affected the wetting time and distribution of PCBs. The molten solder temperature at 523 K demonstrated desirable wetting distribution and yielded a stable fountain profile and was therefore considered the best temperature in this study. The simulation results were substantiated by the experimental results.

Keywords: Wave soldering; Wetting area; Volume of fluid (VOF); Finite volume method; Printed circuit board (PCB).

NOMENCLATURE

Cp	specific heat	η	viscosity
g	gravitational acceleration	ρ	density
k	thermal conductivity	$\dot{\gamma}$	shear rate
p	pressure		
T	temperature		
u	fluid velocity component in x-direction	γ_{gl}	surface tension of liquid
v	fluid velocity component in y-direction	γ_{gs}	surface tension of solid
w	fluid velocity component in z-direction	γ_{ls}	surface tension between liquid and solid
x, y, z	cartesian coordinates		

1. INTRODUCTION

Wave soldering, a traditional soldering technique widely used in electronics assembly processes, was originally developed for attaching through-hole components to printed circuit boards (PCBs). Understanding the process parameters of wave soldering, such as temperature, conveyor speed, soldering angle, pre-heating, and cooling zones, is imperative to achieving optimal process conditions. However, wave soldering machines of different designs (e.g., for low- to high-volume production and various zones) may have different optimum process parameter controls. Therefore, previous studies have applied Design of Experiments (DOE) through experimental testing and regression model (Liukkonen *et al.* 2011) to understand and obtain optimal control of this process.

Several studies have investigated the wave soldering process using experimental studies, finite element analysis, characterization, and optimization. Polsky *et al.* (2000) studied printed wiring board (PWB) warpage resulting from simulated infrared and wave soldering processes. Two types of bare, four-layer PWB test vehicles were developed to simplify the typical boards produced by PWB manufacturers. In the above study, the boards were tested in a small laboratory-scale oven integrated with a shadow Moiré out-of-plane displacement measurement system. Warpage was observed in two different PWB designs after the simulated wave and infrared reflow soldering processes.

Lead-free (Sn/Ag/Cu) wave soldering that enabled environment-friendly and high-volume production was proposed by Baylakoglu *et al*. (2005), who investigated the significance of nitrogen in dross rate reduction, product quality, and process. Dross formation (Sn/Ag/Cu) in a nitrogen environment was compared with eutectic leaded solder (Sn/Pb) bath under an air atmosphere. Board quality was also evaluated on the application of no-clean, volatile organic compound (VOC)-free flux. The researchers found that the application of nitrogen with Sn/Ag/Cu alloy enhances the wave soldering process. In addition, increasing the solid quantity of flux yields better solder joints and minimizes short rates.

Morris and Keefe (2003) investigated the effects of Tin (Sn)-rich solders coming into contact with various materials. The corrosion effects of Sn on various materials (e.g., stainless steels, coated stainless steel, titanium, cast iron, and other materials) were studied. Failed samples were examined using optical and scanning electron microscopy (SEM) and X-ray emission chemical analysis. The resulting analyses indicated that an unprotected stainless steel solder pot was inappropriate for use in Sn-rich solder. Titanium and gray cast iron solder pots were recommended because of their excellent corrosion resistance.

Forsten *et al*. (2000) studied the interactions among the PCB, flux, solder alloy, and processing equipment used in the lead-free wave soldering. Three Sn-rich alloys were used in this investigation: SnAg3.5, SnCu0.7, and SnAg3.8Cu0.7. The researchers found that the oxide layer on top of the SnAgCu alloy is more durable than SnPb. However, drossing rate, lead build up, defect rates, and post-process optimization were the same as those of the previous SnPb process.

An experimental investigation of lead-free wave soldering using 95.5Sn/3.8Ag/0.7Cu alloy was conducted by Arra *et al*. (2002), who performed a DOE considering three variables, namely, solder bath temperature, conveyor speed, and soldering atmosphere, in a dual-wave system and four no-clean flux systems, including alcohol- and water-based types. A "Lead-Free Solder Test Vehicle" was used in these experiments. The water-based flux system was found to be the best fluxing system for various process conditions. The soldering results indicated that optimum flux and process parameters are more important than Sn/Pb in achieving acceptable Sn/Ag/Cu soldering performance.

Liukkonen *et al*. (2009, 2011) focused on the application of self-organizing maps and quality-oriented optimization in the wave soldering process. The solder defect numbers were presented in the data as a measure of product quality, whereas optimization was performed by minimizing a cost function describing the total repair costs of a wave-soldered PCB. The researchers found interesting interactions between certain process parameters and solder defects in the wave soldering process. Moreover, the results clearly showed the potential of optimization, particularly in the visualization of optimal process conditions.

The wave soldering technique has also been applied in advanced filling for through silicon via (TSV). Ko *et al*. (2011) investigated advanced filling technology for three-dimensional (3D) layering on electronic circuits. Wave soldering-vacuum filling was used to fill the molten solder into the TSV of a wafer with a thickness of 100 μm to 200 and hole diameters of 20 μm to 30 μm. Deep reactive ion etching was used to form TSVs. The surface was sputtered by means of a wetting layer of Ti/Cu or Au. In the filling process, vacuum pressure (0.02 MPa to 0.08 MPa), specifically the difference in pressure between the upper and lower parts, facilitated the feeding of molten solder into the TSV holes. The resulting filling speed was less than 3 s, significantly faster than in conventional methods.

Aerosol pollution by electronic companies may harm employees, particularly those in the production line. Szoboszlai *et al*. (2012) examined the elemental composition and mass size distribution of indoor aerosol particles in a wave soldering working environment. The researchers analyzed particle types and characteristics using SEM. The total and regional deposition efficiencies of the different types of particles within the human respiratory system were calculated using a stochastic lung deposition model. The particulate matter and lead concentrations in the working environment were far below World Health Organization guidelines. However, the concentration values were found to increase in the wave solder production area, indicating that human activities affect the total deposition fraction. A higher deposition fraction was found to result from light exercise than from sitting. However, the deposition in the deeper acinar region was found to be higher when sitting.

Suganuma *et al*. (2000) performed a simulation analysis of the lift-off mechanism, which is a type of severe defect formation. This problem occurs when the solder fillet peels off from a Cu land pad on a PWB. In the above study, basic Sn–Bi alloys (Sn at 2 wt% to 5 wt %) and the solidification simulation method were used. The researchers found that the lift-off problem resulted from the rapid solidification of the solder fillet, which propagates from a lead wire to a fillet edge. This problem was mitigated through rapid cooling and

annealing at high temperature.

Franken *et al*. (2000) performed a finite element analysis of the failure possibility of ceramic multilayer capacitors in wave soldering and bending loads. A two-dimensional numerical analysis was performed to predict the reliability of multilayer capacitors. Preheating and soldering temperatures were found to be greater factors in failure probability than the thickness of the nickel layer, soft solder geometry, and the number of inner electrodes. Proper control of preheating and soldering temperatures in wave soldering can yield optimal product reliability.

Generating wave solders at various temperatures may affect the wetting of the component pin/interconnector within the PCB, which may consequently lead to poor reliability and product rejection. Wetting behavior and the molten solder in the assembly process are essential to the capability of the microelectronic industry to maintain the reliability and quality of the product. In addition, the simulation tool provides a detailed visualization and better understanding of the process.

In this study, simulation and experimental analyses were conducted at different molten solder temperatures to visualize and investigate the mechanism of solder wave distribution on the PCB during the assembly process. As far as the authors are aware, the literature on wetting and wave solder behavior analysis using simulation/modeling remains limited. Thus, this research gap is ameliorated by the current study, which models a 3D wave soldering machine considering the effects of wave solder temperature and wetting profiles. FLUENT 6.3.26 software was used to simulate molten solder flow during the assembly process. The flow front was tracked using the volume of fluid (VOF) model. The predicted results were validated by the experimental results.

2. GOVERNING EQUATIONS

This study focuses on fountain formation at the soldering (assembly) stage and on the PCB. The fountain flow was analyzed using the FLUENT solver. In the FLUENT analysis, the flow behavior of the molten solder fountain was described using governing equations. The soldering pot and the outer region were considered by the simulation model, where the soldering pot contained molten solder. Thus, the solder bath was defined as the fluid domain in the analysis, whereas the soldering pot was initially defined with molten solder. FLUENT was utilized to solve the governing equations during the wave soldering process. The continuity equation, which is suitable for incompressible flow, is expressed as:

$$\frac{\partial u}{\partial x}+\frac{\partial v}{\partial y}+\frac{\partial w}{\partial z}=0 \tag{2}$$

where u, v, and w are the velocity vectors in the x, y, and z directions, respectively. The momentum conservation equation for 3D Newtonian fluids is expressed as (Ong et. al 2012b):

$$\rho\left(\frac{\partial u_i}{\partial t}+u\frac{\partial u_i}{\partial x}+v\frac{\partial u_i}{\partial y}+w\frac{\partial u_i}{\partial z}\right)=-\frac{\partial P}{\partial i}$$
$$+\mu\left(\frac{\partial^2 u_i}{\partial x^2}+\frac{\partial^2 u_i}{\partial y^2}+\frac{\partial^2 u_i}{\partial z^2}\right)+\rho g_i \tag{3}$$

Where i represents x, y and z directions, ρ is the fluid density, P is the static pressure, μ is the fluid viscosity, and g is the gravitational acceleration.

The energy conservation equation is expressed as (Ong et. al 2012a):

$$\rho C_p\left(\frac{\partial T}{\partial t}+u.\nabla T\right)=\nabla(k\nabla T) \tag{4}$$

where k is the thermal conductivity, Cp is the specific heat, and T is the temperature. To track the free surface of the leaded molten solder (Sn63Pb37) and air, VOF was used in the analysis. The equation of melt front over time is described as (Khor et. al 2011):

$$\frac{dF}{dt}=\frac{\partial F}{\partial t}+\nabla.(uF)=0 \tag{5}$$

The basic concept of VOF is to allocate the liquid phase by assigning each cell in the computational domain. F denotes the volume fraction of the cell occupied by liquid. Thus, F = 1 represents the cells filled only by molten Sn63Pb37 (in red color), F = 0 represents the cells void of compound (in blue color), and 0 < F < 1 represents interface cells or the melt front of Sn63Pb37.

In wave soldering, the PCB with the appropriate components passes through the soldering pot. The interaction between the molten solder from the pot and the solid surface (the bottom surface of PCB) creates a metallurgical bond. The capability of Sn63Pb37 to flow and spread over the PCB during wave soldering is an important criterion for the formation of the appropriate metallic bond. This phenomenon is referred to as "wetting," which is defined as the capability of a liquid to spread over another material, generally a solid (Wassink and Verguld, 2000). Wetting is measured based on the contact angle between the solid and the liquid in a particular environment, as illustrated in Fig. 1. The system is wet if the contact angle lies between 0° and 90°, but is considered non-wetting if the contact angle is between 90° and 180°. The wetting angle is affected by surface roughness, time, flux effectiveness, and ambient temperature.

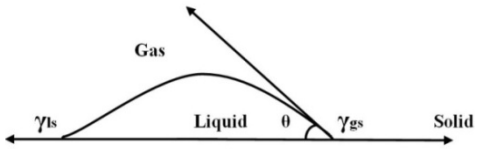

Fig. 1. Wetting angle.

Based on the Young–Dupre equation, contact angle θ is expressed as the balance of the surface tension at the junction (Mulugeta and Guna, 2000):

$$\gamma_{gs}=\gamma_{ls}+\gamma_{gl}\cos\theta \tag{6}$$

where γ_{gs} is the surface tension of a solid in a

particular environment, γ_{ls} is the surface tension (interfacial energy) between liquid and solid, and γ_{gl} is the liquid surface tension in the same environment.

The surface tension among Sn63Pb37, the flux, and the substrate affects the degree of wetting. Previous research reported that the surface tension of solder material varies with temperature (Howie and Lea, 1984). However, this study only focused on the visualization of the solder wave profile and the molten solder spreading time over PCB at various Sn63Pb37 temperatures. Given that the surface of the PCB was assumed to be fully wetted by flux, fluxing was disregarded in this study.

3. EXPERIMENTAL SETUP

Prior to the simulation study, an experiment was conducted to validate the feasibility of predicted results by comparing them with the experimental results. An appropriate experiment was conducted using a leaded/lead-free wave soldering machine to study the fountain formation, molten solder distribution, and wetting characteristics of PCB. The dimension of PCB used in the experiment was 146 mm × 70 mm × 2.0 mm, as illustrated in Fig. 2. The experiment was set up as shown in Fig. 3. The leaded/ lead-free wave soldering machine consists of four main zones: the fluxing, preheating, soldering, and cooling zones. The solder pot temperature is controllable within the range of 456 K to 643 K. A suitable speed of the solder pump was selected to ensure a particularly smooth and stable solder wave during soldering.

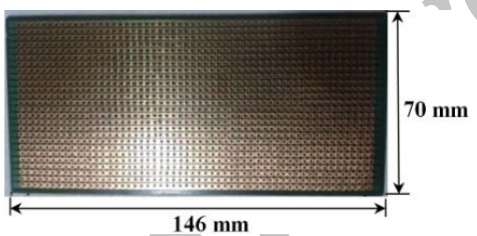

Fig. 2. Line printed circuit board (PCB).

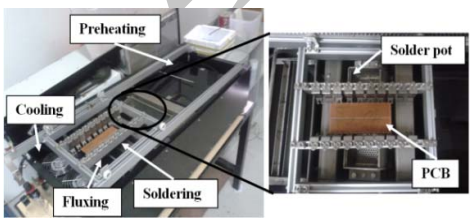

Fig. 3. Leaded/ lead free wave soldering machine.

The current study focused on the wave soldering zone to visualize the solder wave and wetting profile during the process. The solder pot section was filled with 56 kg of Sn63Pb37, and the temperature was set to 456 K < T < 643 K. The propeller speed of the solder pot was set at 830 rpm to generate a solder wave, as commonly practiced in the electronics industry. The wave and wetting profile were recorded using a video camera showing the bottom view of the PCB and the front view of solder pot. The profile of the lined PCB and the image of the wave soldering machine used in the present experiment are shown in Figs 2 and 3, respectively.

4. SIMULATION MODELING AND MATERIAL PROPERTIES

In the simulation set-up, the geometry of the solder pot, which consisted of a six-bladed propeller, and the PCB were constructed to analyze the effect of temperature on the wetting profile of the PCB. In this study, Sn63Pb37 was used as the solder material under various temperatures (i.e., 456 K, 473 K, 523 K, 583 K, and 643 K). The CFD pre-processing software was utilized for the geometrical modeling, meshing, and boundary condition set-up. The computational domain (225 mm × 510 mm × 210 mm), which consisted of the solder pot and the propeller, was developed. Figs. 4 and 5 show the modeling computational domains including the solder pot, the outer domain, and the PCB for the present study.

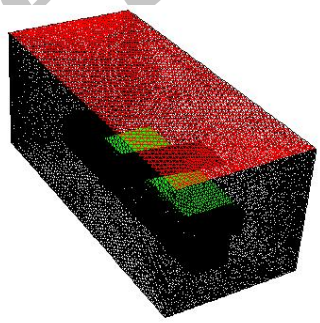

Fig. 4. Meshed model.

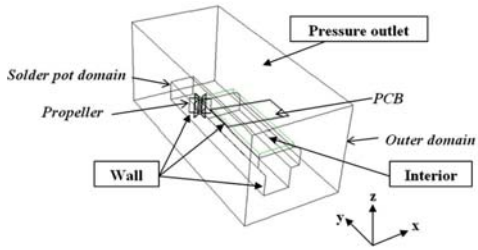

Fig. 5. Boundary condition of the simulation.

FLUENT (Bandyopadhyay and Das, 2013) (Abdul Aziz *et al.* 2013, 2014 a, b) is the commercial finite volume (FV)-based software used for fluid analysis. The model constructed using CFD pre-processing software was uniformly meshed with 586852 tetrahedral/ hybrid elements. This model was later exported as a meshed model for the fluid solver. FLUENT was used for further analysis. The propeller speed induced the turbulence flow of the molten solder from the solder pot to the PCB. Thus, the turbulence model of K-epsilon Realizable was

considered in the governing equations. Moreover, the combination of the fine mesh around the wall (solder pot and PCB) and the fluid flow were in perfect condition for the viscous model, particularly throughout the viscous-affected region.

In the FLUENT setting, the SIMPLE algorithm was applied for pressure–velocity coupling. An optimum time step of 0.001 s and a second-order upwind scheme setting were used in the simulation. The under relaxation factors for the modified turbulent pressure, density, and momentum were 0.3, 1, and 0.2, respectively. To analyze the fluid flow accurately, an optimum time step is required for a transient/ unsteady case. Different time steps were examined to obtain the optimum time step size. Finally, 0.001 s was found to be the optimum time step size for the current simulation. This result required approximately 10 000 iterations, which corresponded to approximately 12 h of computing time per case using a computer with 2.0 GB memory and 3 GHz processor.

In this study, the surface of the PCB, the solder pot, and the outer domain were defined as the wall boundary. The outer solder pot and domain were defined as the interior and the pressure outlet, respectively. Therefore, the boundary and initial conditions for computational analysis are (Khor et. al 2011):

(a) On wall : $u=v=w=0;\ T=Tw,\ \frac{\partial p}{\partial n}=0$

(b) On melt front : $p = 0$

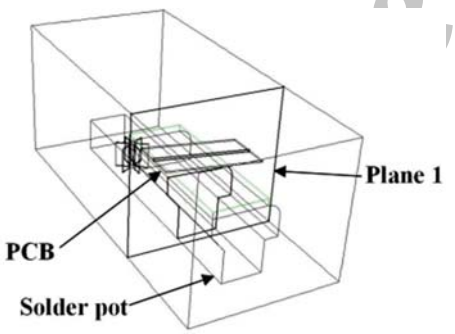

Fig. 6. Cross-sectional view of wave soldering pot and PCB at Plane 1.

Table 1 Sn63Pb37 Thermal properties (Shen *et al.* 2005)

Density (kg/m^3)	8510
Specific Heat capacity, Cp (J/kg-k)	183
Thermal Conductivity (W/m-k)	53

The solder pot temperature was set at different temperatures (456 K, 473 K, 523 K, 583 K, and 643K) accordingly for melting Sn63Pb37. Two phases of fluid (air and Sn63Pb37) were defined in the analysis, and the molten solder was generated at a propeller speed of 830 rpm. The solder material properties are summarized in Table 1. In addition, the cross-sectional view of the solder pot and the PCB within Plane 1 is shown in Fig. 6, which illustrates the wetting and molten solder fountain profile of the PCB at various temperatures. The predicted results were verified using the solder wetting image obtained in the experiment.

5. MESH-DEPENDENCY SOLUTION

Grid independence analysis was performed to obtain the optimum mesh size. Table 2 presents the summary of mesh-dependency solution and computing time for each case after 2.5 s. The different mesh sizes tested and the corresponding percentages of the wetting area with respect to time are illustrated in Fig. 7. These meshes were referred to as Mesh I, Mesh II, Mesh III, Mesh IV, Mesh V, and Mesh VI corresponding to 1.08×10^5, 2.37×10^5, 3.65×10^5, 4.32×10^5, 5.87×10^5, and 7.13×10^5 elements, respectively. The time step size was set as 1×10^{-3} s. Mesh VI had finest grid size. The deviations in the percentage of wetting areas for Cases I to V were compared with Case VI. A courser number of nodes or elements were found to exhibit significant variations. Mesh V and mesh VI were better, with a nominal deviation of 0.21% between them. Therefore, Mesh V was selected as the optimum in terms of accuracy and computational cost. Fig. 7 shows the minimum deviation between Cases V and VI. Both cases exhibited a wetting area and trend that were similar to each other, unlike Cases I to IV.

Table 2Mesh size for mesh-dependency solution

Mesh	I	II	III
Elements	108276	236754	365197
Wetting area %, at filling time, t=2.5s	50.32	47.14	45.64
Deviation from mesh VI	7.55	4.37	2.87
Computing time	58 hours	65 hours	74 hours

Table 2 Mesh size for mesh-dependency solution (cont)

Mesh	VI	V	VI
Elements	432163	586852	712734
Wetting area %, at filling time, t=2.5s	43.92	42.98	42.77
Deviation from mesh VI	1.15	0.21	0.00
Computing time	83 hours	96 hours	131 hours

6. RESULTS AND DISCUSSION

6.1 Experimental Validation at Full Wetting for *T= 523 K*

The wetting area of the PCB is crucial during wave soldering because it may affect the reliability and

strength of the PCB components. The fountain of molten solder interacts with the PCB that passes through the solder pot, resulting in the wetting of the PCB. As previously mentioned in Section 3, the experimental result of the PCB wetting area was compared with the predicted simulation result at a molten solder temperature of 523 K. Fig. 8 illustrates the predicted wetting area using the current simulation and the result obtained from the experiment. In this study, the wetting profile and area were evaluated against both the simulation and experimental results. Fig. 8 (b) shows the comparison between the solder wetting profiles for both simulation and experiment. Both results showed nearly identical wetting profiles. The percentage of the wetting area relative to the whole PCB area is presented in Table 3. The deviation for both results was only 5.24%.

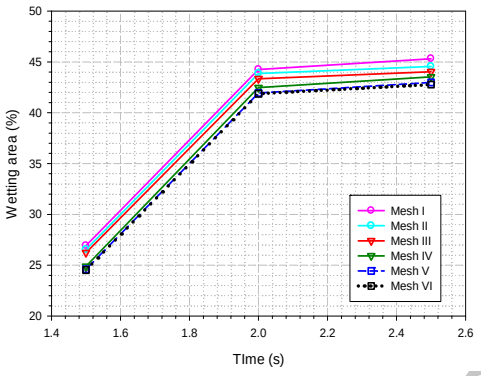

Fig. 7. Mesh-dependency solution; Wetting area (%) vs. wetting time (s).

Table 3Solder wetting area and discrepancy for both simulation and experiment

Result	Area (cm^2)	Wetting (%)	Discrepancy (%)
Simulation	85.19	90.26	5.24
Experiment	90.13	95.50	

Fig. 9 illustrates the comparison between the wetting length of the PCB and fountain advancement in the current experiment. Reference lines of the soldering pot were labeled in Fig. 9 (a). Fig. 9 (b) shows the molten solder fountain profile, wetting length (A), and maximum fountain advancement (B). The fountain had almost similar shape for both simulation and experiment. Moreover, the wetting length and fountain advancement were determined, as shown in Fig. 9 (c). The lengths of wetting and fountain advancement for the simulation and experiment had discrepancies of only 9.74% and 8.00%, respectively. These results demonstrated the capability of the simulation tool in handling the wave soldering process. Therefore, the current study is extended to include the effect of temperature on the solder wetting profile.

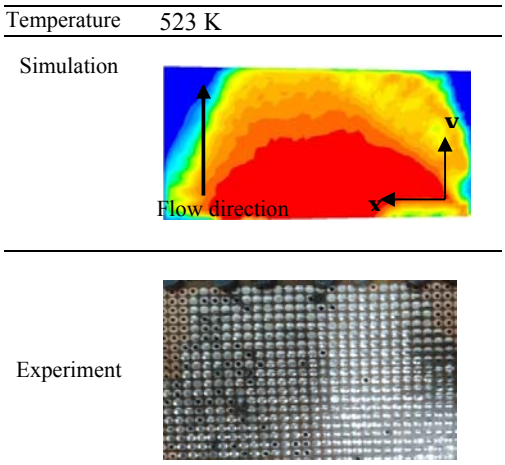

(a) Simulation contour and experimental solder area.

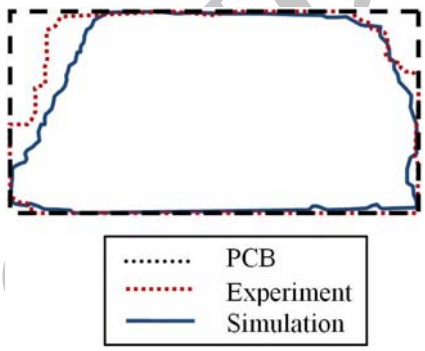

PCB area = 94.38 cm^2

(b) Solder wetting profile for simulation and experiment.

Fig. 8. Comparison of simulation and experimental results.

6.2 PCB Wetting Profile

Various solder pot temperatures ranging from 456 K to 643 K were considered in the current simulation analysis. The wetting profiles of the PCB at different solder pot temperatures were compared and presented at 1.5 s, 2.0 s, and 2.5 s, as shown in Fig. 10. From the simulation results, the wetting area of the PCB increased as time increased, wherein the profile propagated in the y direction. This situation was attributed to the generated fountain profile in the solder pot. The fountain of the molten solder was generated by the propeller in the solder pot until the fountain advancement was sufficient to interact with the bottom surface of the PCB. At the same time, the electronic components were assembled to the PCB. Poor wetting profile and insufficient wetting area of the PCB may affect the joining of the component. Thus, appropriate parameters, such as temperature control, are important in the wave soldering process.

(a) Solder pot (Limits of level XYZ for solder fountain formation).

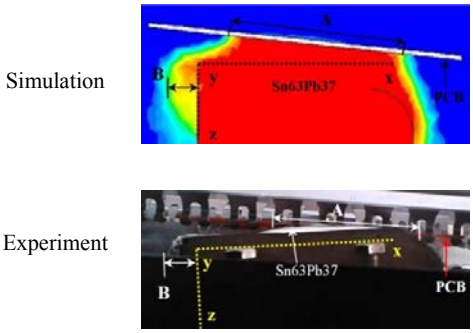

(b) Contour comparison from side view. (Note: A-PCB wetting distance; B-Maximum fountain advancement).

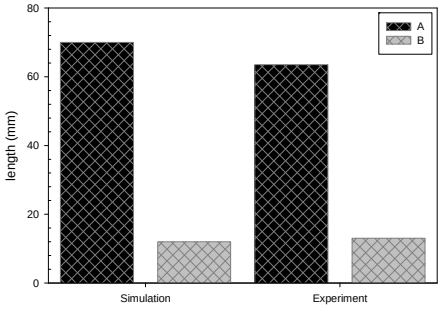

(c) Sn63Pb37 solder advancement; A-PCB wetting distance, B-maximum fountain advancement.

Fig. 9. Wetting length and fountain advancement of molten solder during the experiment.

In the simulation analysis, the solder pot temperature significantly influences the wetting profile. Increase in temperature resulted in an uneven wetting profile. At a high temperature, the viscosity of molten solder was low and induced an unstable fountain formation, resulting in an uneven wetted area (with a volume fraction less than 0.5) on the PCB. This result is clearly shown in Fig. 10 at 583 K and 643 K, which is unlike that of the wetted area at 523 K. The wetting area of the PCB, which varied with time, is plotted in Fig. 11. Fig. 11 clearly shows the effect of temperature on the wetting area. Although a high temperature yielded higher percentage of wetting area, it was not the best temperature for the wave soldering process because a high temperature resulted in an uneven wetted area, as clearly shown in Fig. 10. Therefore, better understanding of the parameter control of wave soldering can yield the targeted product quality.

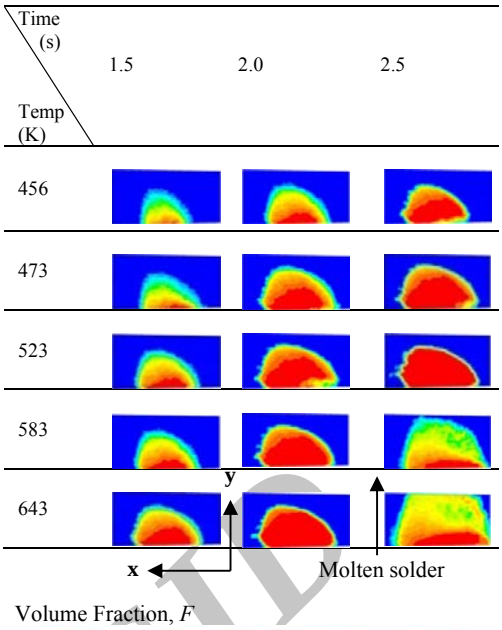

Fig. 10. PCB profile (bottom view).

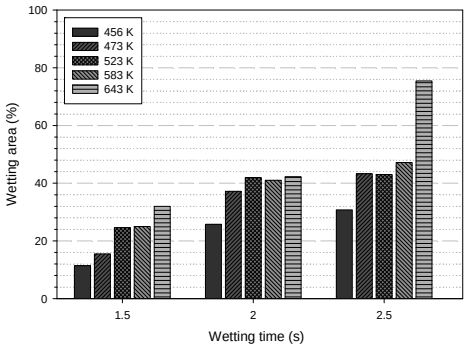

Fig. 11. Wetting area (%) vs. wetting time (s).

6.3 Velocity Vector (phase) at Full Wetting

Full wetting of PCB occurs when the fountain of the molten solder material of the solder pot reaches and interacts with the bottom surface of the PCB. A center plane that was defined at the domain and discussed in Section 4 was utilized to study the velocity vector of the fountain that interacted with the bottom surface of the PCB during wave soldering. The velocity and contour profiles for different solder pot temperatures are presented in Fig. 12. From the contour profile, the fountain shapes, as well as the velocity vectors, at 456 K and 473 K were almost similar. When the temperature increased from 523 K to 643 K, the fountain profile and the concentration of the velocity vector changed. The increase in temperature resulted in the decrease of molten solder viscosity. In addition, the continuous fountain generated by the propeller had caused instability in the fountain. More wave forms were likewise created when the viscosity of molten

solder was low. Fig. 12 clearly shows the velocity vector at 643 K, wherein the velocity vectors of the molten solder were non-uniformly distributed unlike the others. From this point of view, the increase in the solder pot temperature significantly affected the distribution of velocity vectors and resulted in the unintended wetting performance.

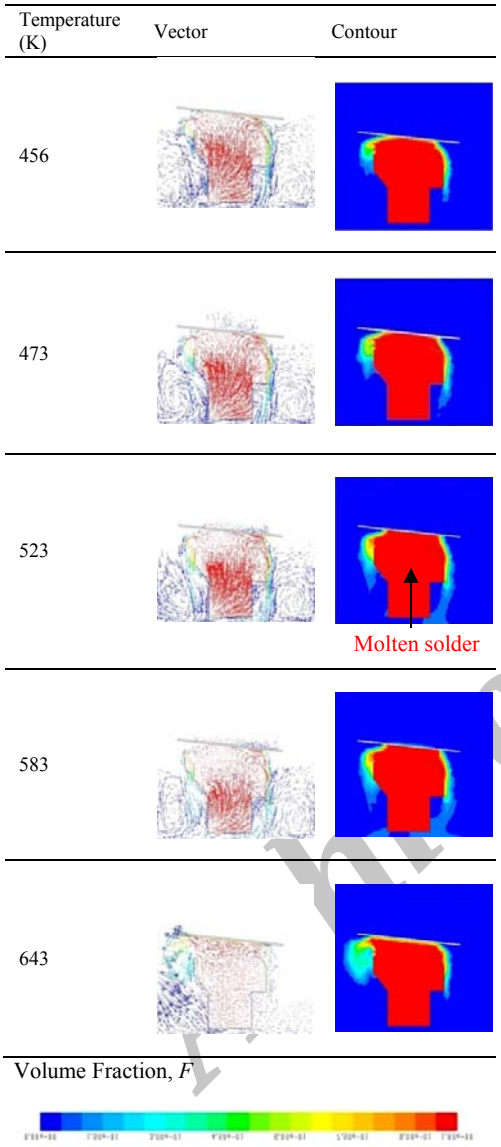

Fig. 12. Velocity vector at full wetting.

6.4 PCB Profile at Full Wetting

Fig. 13 shows the predicted PCB wetting profile when using different solder pot temperatures. Moreover, Fig. 13 shows that different temperature settings caused various wetting profiles on the PCB, and that the time to achieve full wetting varied with each temperature as well. Based on the results, the increase of solder pot temperature during wave soldering caused a dispersed and uneven pattern of the wetting area. The volume fractions for the 583 K and 643 K cases were lower than for the 523 K case. Moreover, at 523 K, the wetting of the molten solder on the PCB showed better distribution than in other cases. This situation revealed that temperature control is important in wave soldering, in such a way that temperature affects the percentage of the wetting area (Fig. 14) and the time (Fig. 15) to achieve full wetting on the PCB. The correlation between the percentage of wetting area and temperature is plotted in Fig. 14. The most suitable temperature setting to obtain a higher wetting area on the PCB for the current wave soldering was 523 K. However, lower temperature (< 523 K) and higher temperature (> 523 K) did not yield better wetting performances. This condition may be attributed to the variation of molten solder viscosity which corresponded to the solder pot temperature. Moreover, wetting time was also affected by the increase in temperature. Wetting time decreased as temperature increased, as illustrated in Fig. 15.

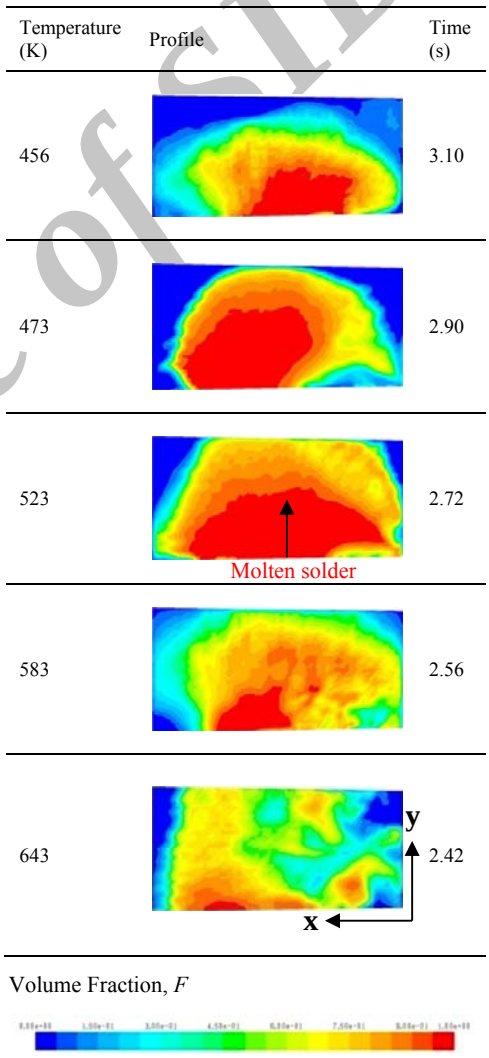

Fig. 13. PCB profile (bottom) atfull wetting.

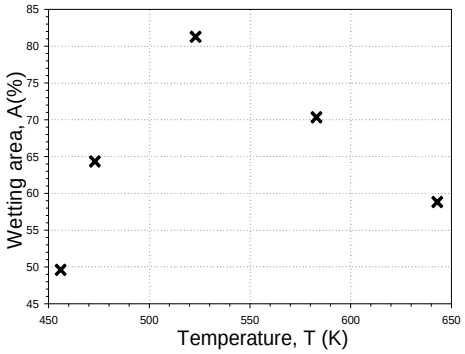

Fig. 14. Wetting area (%) vs. Temperature (K)atfull wetting time.

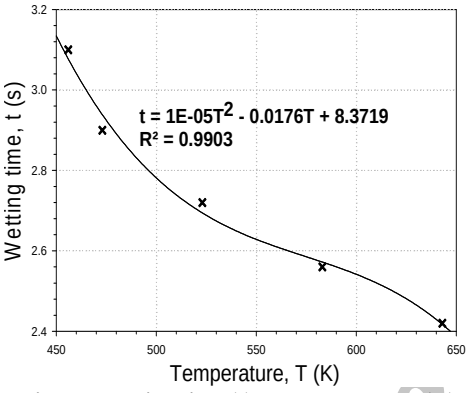

Fig. 15. Wetting time (s) vs. Temperature (K).

7. CONCLUSIONS

This study investigated the effects of temperature on wave soldering of PCBs using three-dimensional FV-based simulation. The temperature of the solder pot is important in wave soldering, which significantly affects the wetting pattern, wetting area, and wetting time of the PCB, as well as the molten solder behavior during fountain formation. This study showed that a solder pot temperature of 523 K yields better performance compared with temperatures ranging from 456 K to 643 K. At 523 K, a stable and higher full wetting area can be obtained during wave soldering and an approximately 90% wetting area can be achieved. Although a short wetting time of the PCB can be attained at a high solder pot temperature, such temperature can result in an irregular and dispersed wetting pattern on the PCB. Therefore, the optimum temperature setting for the wave soldering process is crucial for a better wetting performance of the PCB. The results with regard to the predicted wetting area were substantiated by current experimental results. Thus, this study demonstrated the excellent capability of FLUENT in solving and predicting the wave soldering process. The current results are useful as the reference for the engineer and researcher in the PCB assembly industry.

ACKNOWLEDGEMENTS

The author gratefully acknowledges the financial support of the Ministry of Higher Education of Malaysia, and the My Brain 15 PhD scholarship program.

REFERENCES

Abdul Aziz, M. S., M. Z. Abdullah and C. Y. Khor (2014a). Influence of PTH offset angle in wave soldering with thermal-coupling method, *Soldering & Surface Mount Technology* 26(3), 97-109.

Abdul Aziz, M. S., M. Z. Abdullah, C. Y. Khor and F. Che Ani (2013). Influence of pin offset in PCB through-hole during wave soldering process: CFD modeling approach, *International Communications in Heat and Mass Transfer* 48, 116-123.

Abdul Aziz, M. S., M. Z. Abdullah, C. Y. Khor, A. Jalar and F. Che Ani (2014b). CFD modeling of pin shape effects on capillary flow during wave soldering, *International Journal of Heat and Mass Transfer* 72, 400-410.

Arra, M., D. Shangguan, S. Yi, R. Thalhammer and H. Fockenberger (2002). Development of lead-free wave soldering process, *IEEE Transactions on Electronic Packaging Manufacturing* 25(4), 289-299.

Bandyopadhyay, T. K. and S. K. Das (2013). Non-Newtonian and Gas-non–Newtonian Liquid Flow through Elbows – CFD Analysis,*Journal of Applied Fluid Mechanic* 6(1), 131-141.

Baylakoglu, I., S. Hamarat, H. Gokmen and E. Meric (2005). Case study for high volume lead-free wave soldering process with environmental benefits, ISEE, 102-106.

Fosten, A., H. Steen, L. Willding and J. Friendrich (2000). Development and validation of lead-free wave soldering process, *Soldering and Surface Mount Technology* 12(3), 29-34.

Franken, K., H. R. Maier, K. Prumeand, R. Waser (2000). Finite element analysis of ceramic multilayer capacitor: Failure probability caused by wave soldering and bending loads, *Journal of the American Ceramic Society* 83(6), 1433-1440.

Howie, F. H. and C. Lea (1984). Blowholing in PTH solder fillets-towards a solution, *Proceedings of INTERNEPCON UK*, Brighton, 104-111.

Khor, C. Y., M. K. Abdullah, M. Z. Abdullah, M. A. Mujeebu, D. Ramdan, M. F. M. A. Majid and Z. M. Ariff (2011). Effect of vertical stacking dies on flow behavior of epoxy molding compound during encapsulation of stacked-chip scale packages, *Heat and Mass Transfer* 46(11-12), 1315-1325.

Ko, Y. K., H. T. Fuji, Y. S. Sato, C. W. Lee and S.

Yoo (2011). Advanced Solder TSV Filling Technology Developed with Vacuum and Wave Soldering, *Electronic Components and Technology Conference*, IEEE, Lake Buena Vista, FL, 2091–2095

Liukkonen, M., E. Havia, H. Leinonen and Y. Hiltunen (2009). Application of self-organizing maps in analysis of wave soldering process, *Expert Systems with Application* 36, 4604-4609.

Liukkonen, M., E. Havia, H. Leinonen and Y. Hiltunen (2011). Quality-oriented optimization of wave soldering process by self-organizing maps, *Applied Soft Computing* 11, 214-220.

Morris, J. and M. J. O. Keefe (2003). Equipment Impacts of Lead Free Wave Soldering, *APEX 2003,* Camdenton, MO.

Mulugeta, A. and S. Guna (2000). Lead-free Solders in Microelectronics, *Materials Science and Engineering* 27, 95-141.

Ong, E. E. S., M. Z. Abdullah, C. Y. Khor, W. K. Loh, C. K. Ooi and R. Chan (2012a). Analysis of encapsulation process in 3D stacked chips with different microbump array, *International Communications in Heat and Mass Transfer* 39, 1616-1623.

Ong, E. E. S., M. Z. Abdullah, W. K. Loh, C. K. Ooi and R. Chan (2012b). FSI implications of EMC rheological properties to 3D IC with TSV structures during plastic encapsulation process, *Microelectronics Reliability* 63(4), 600-611.

Polsky, Y., W. Sutherlin and U. I. Charles (2000). A comparison of PWB warpage due to simulated infrared and wave soldering processes, *IEEE Transactions on Electronics Packaging Manufacturing* 23(3), 191-199.

Shen, L., M. Wang, Y. He, T. F. Lam and Y. Q. Jiang (2005). Reflow profile simulation by finite element method for a BGA package,*Proceeding of Electronic Packaging Technology, 2005 6th International Conference*, 30 August-2 September, 419-422.

Suganuma, K., M. Ueshima, I. Ohnaka, H. Yasuda, J.Zhu and T. Matsuda (2000). Lift-off Phenomenon in Wave Soldering, *Acta Metallurgica* 48, 4475-4481.

Szoboszlai, Z., Z. Kertesz, S. Szikszai, A. Angyal, E. Furu, Z. Torok, L. Daroczi and A. Z. Kiss (2012). Identification and chemical characterization of particulate matter from wave soldering processes at a printed circuit board manufacturing company, *Journal of Hazardous Materials* 203-204, 308-316.

Wassink, K. J. R. and M. M. F. Verguld (2000). Manufacturing Techniques for Surface Mounted Assemblies'', *Electrochemical Publications Ltd*., GB-Port Erin, British Isles, 17.